Directed Evolution of Replication-Competent dsDNA Bacteriophage towards New Host Specificity

Jing Liang[1], Huibin Zhang[2], Yee Ling Tan[1], Huimin Zhao[3,*], and Ee Lui Ang[1,*]

[1] Strain Engineering, Singapore Institute of Food and Biotechnology Innovation, Singapore 138669, Singapore.

[2] Metabolic Engineering Research Laboratory (MERL), Agency for Science, Technology, and Research (A*STAR), Singapore, 138669, Singapore.

[3] Department of Chemical and Biomolecular Engineering, University of Illinois at Urbana-Champaign, Urbana, IL 61801, United States.

***** To whom correspondence should be addressed. H.Z. (email: zhao5@illinois.edu) and E.L.A. (email: ang_ee_lui@sifbi.a-star.edu.sg)

ABSTRACT

In the fight against antimicrobial resistance, bacteriophage is a promising alternative to antibiotics. However, due to their narrow spectrum, phage therapy requires the careful matching between host and bacteriophage to be effective. Despite our best efforts, nature remains as the only source of novel phage specificity. Directed evolution can potentially open an avenue for engineering phage specificity and improving qualities of phages that are not strongly selected for in their natural environments but are important for therapeutic applications. In this work, we present a strategy that generates large libraries of replication-competent phage variants directly from synthetic DNA fragments, with no restriction on their host specificity. Using the T7 bacteriophage as a proof-of-concept, we created a large library of tail fiber mutants with at least 10^7 unique variants. From this library, we identified mutants that has broadened specificity as evidenced by their novel lytic activity against *Yersinia enterocolitica*, a strain that the wild-type T7 was unable to lyse. Using the same concept, mutants with improved lytic efficiency and characteristics, such as lytic condition tolerance and resistance suppression, were also identified. However, the observed limitations in altering host specificity by tail fiber mutagenesis suggests that other bottlenecks could be of equal or even greater importance.

KEYWORDS

Phage engineering, directed evolution, phage specificity, synthetic phage platform, tail fiber engineering

INTRODUCTION

With the growing threat of antimicrobial resistance (AMR) and the lack of adequate drugs in the pipeline, AMR infection is poised to overtake cancer as the leading cause of death by 2050, resulting in the loss of 10 million lives and US$8 trillion in GDP annually [1,2]. Phage therapy has been identified as one of the most promising alternatives currently on the horizon, and recent successes have prompted renewed interest in harnessing the potential of this century-old practice [3–6].

One of the key limitations in phage therapy has been the host-specificity of phages. Being highly host-specific, phages tend to be narrow-spectrum, and require careful matching to the specific infection [6]. Current treatment strategy often relies on the screening of a large library of characterized phage isolates in multiple phage banks to find ones that work for the specific infection [5,7,8]. This requirement makes phage therapy resource-intensive and expensive. Furthermore, being overly specific also allows the host to readily evolve resistance towards any given phage, which invariably occurs [9]. If resistance occurs before therapeutic effect is achieved, a re-screening for new phages may become necessary. Furthermore, as phages rely on their hosts for replication, highly effective phages that are too effective in killing their hosts would have gone extinct in nature. However, highly effective phage is exactly what we desire in phage therapy.

In an attempt to address this limitation, various groups have developed strategies to artificially adapt phages to new hosts [10,11]. However, these strategies require the availability of a phage that can invade the target strain – i.e. we need to know the solution to the problem before we can solve it. In addition, because they are natural isolates, we cannot expect the resultant phages to be 100% efficient. More recently, Dunne et al. and Yehl et al. reported the use of targeted and random mutagenesis to expand the host range of tailed phages [12,13]. However, because Yehl et al. relied on the native host for library preparation, it requires that the resultant library, however diverse, must retain their specificity towards the native host. Variants that resulted in a complete switch in specificity will be lost. While Dunne et al. circumvented the problem through direct genome transfection, the transformation efficiency would limit the library size for many hard-to-transform wild-type strains.

In this work, we aim to unleash the full power of directed evolution to supercharge the capabilities of these host adaptation systems and to enable large phage library preparation

without the need to maintain native host compatibility [14–16]. To enable the rapid engineering and evolution of replication-competent phages with new host specificity, we designed a versatile Golden Gate-based assembly platform to synthesize the phage genomes from synthetic DNA fragments. These synthetic phage genomes can have features that allow for the rapid high efficiency swap-in of mutagenized fragments, and the resultant genomic libraries can be rebooted by cell-free transcription and translation (TXTL), thereby eliminating the need for the library variants to infect the native host.

Using this platform and T7 phage as a model, we generated large random mutagenesis libraries targeting 3 tail component proteins – minor tail protein gp11, major tail protein gp12, and tail fiber gp17 – with 5-8 nt changes per gene, and screened the variant libraries against new strains and species that are resistant to wild-type T7 phage. The tail components are needed for host attachment and are thought to be important determinant of host specificity. We further showed that directed evolution can be used to improve the lysis as well as anti-resistance performance of phages.

RESULTS

Recoding and chemical synthesis of phage T7Syn

To enable Golden Gate assembly, we recoded the T7 phage by removing all *Bsa*I and *Esp*3I sites within protein coding sequences by making synonymous codon substitutions. Sites that are in regulatory regions were removed by making a single A to G substitution. In total, 46 substitutions and a single 13-bp insertion were made. The new genome was then chemically synthesized by a commercial vendor in 14 fragments and cloned into plasmids. Fragments that were toxic to *E. coli* were propagated in yeast plasmids. A list of fragments used for the assembly can be found in Table S8. Similar effect can be achieved via a 52-fragment assembly as demonstrated by Pryor et al.[17]. After sequencing confirmation, the fragments were amplified by PCR and assembled, using a single-step Golden Gate (GG) reaction, into a complete phage genome. The genome was then rebooted via a cell-free transcription translation (TXTL) reaction, and plated onto an *E. coli* BL21 bacterial lawn for plaque formation and isolation (Figure 1A). More than 10^4 plaque forming units (pfu) were obtained from a 12 µL TXTL reaction.

To confirm that the plaques were from the recoded phages, we PCR amplified a heavily recoded fragment from 8 different randomly selected plaques, and digested it using *Bsa*I. All

8 amplicons could not be digested by *Bsa*I, whereas the amplicons from the wild-type T7 phage (T7wt) showed clear signs of digestion (Figure 1B). This shows that the complete T7 genome could be assembled and rebooted at high efficiency.

We performed extensive comparison between the synthetic T7 phage named T7Syn and the wild-type T7 phage to ensure that our recoding did not affect the host range and the propagation of the phage. Using a liquid lysis assay on 47 different strains, we found that T7Syn has the same host range as T7wt (Figure 1E). The burst time (Figure 1D) and resultant final titer (Figure 1C) of T7Syn were found to be identical to that of T7wt. The complete T7Syn genomic sequence as confirmed by next generation sequencing (NGS) is available at GenBank MW248381.

Reassembly and functionalization of T7Syn

T7Syn was then used as the template to generate a diversity of variants. Insertion, deletion, re-arrangement, substitution, and mutagenesis, can all be accomplished easily by PCR using the appropriate primers, followed by Golden Gate assembly and TXTL rebooting. The resultant pfu is inversely related to the number of fragments in the reassembly. From one 12 µL TXTL reaction, we could obtain around 10^5 pfu for a 6-fragment assembly, and up to 10^7 pfu for a 3-fragment assembly, when titered on *E. coli* BL21.

To prepare for the mutagenesis of gp11, gp12, and gp17, we reintroduced *Bsa*I sites flanking those genes – gp11 and gp12 as one cassette, and gp17 as another cassette. The restriction sites were reintroduced by PCR, and the variants were assembled using Golden Gate assembly. As the N-terminal end of gp17 is involved in the phage assembly, we targeted only the C-terminal end (175-553) for mutagenesis. Three variants were made: (1) T7Syn-1112Bs has *Bsa*I site inserted before Gp11 and after Gp12, (2) T7Syn-17Bs has *Bsa*I site introduced at amino acid position 175 of Gp17 by synonymous base substitution, and has *Bsa*I site inserted in the intergenic region after Gp17 (Figure 2A), (3) T7Syn-111217Bs is a combination of the first two variants that allows double substitution (GenBank MW248382). After plaque isolation, the genomic DNA of the phage variants was extracted from high titer lysates. Restriction digestion of the genomic DNA by *Bsa*I confirmed that *Bsa*I sites have been successfully introduced at the expected sites (Figure 2B). The purified genomic DNA was then used as the 'backbone' for subsequent Golden Gate reactions to swap in engineered or mutagenized tail components. Some *Bsa*I modifications affected phage propagation as evident in a delayed burst

time (Figure 2C). However, for most cases, the effect would not impact their application since swapping in a component by Golden Gate (GG) reactions removes the *Bsa*I modifications. If avoiding such handicap is important, special care needs to be taken for modifications that are within intergenic regions, where many regulatory regions reside.

Generation of large high diversity libraries

Because of the potential amplification that could occur during the TXTL reaction, we needed to ascertain that the observed pfu after TXTL was a true representation of library size. We designed an experiment to measure the library size of our reaction by tag sequencing. First, *Bsa*I sites flanking gp17 were introduced together with a 19bp insertion at the 3' end to simulate the effect of a barcode tag (Figure 2A). As the insertion was within the intergenic region of a polycistronic operon, the insertion led to the disruption of the following gene, which affected the propagation of the resultant phage. Our first attempt resulted in a phage that had a slower replication cycle than wild type phages (Figure 2C, T7Syn-17TagBs). Since we needed to minimize the effect of the tag on phage propagation so as to reduce the amount of bias, we padded the insertion with longer T7Syn sequences, which fully reversed the burst time delay (T7Syn-17Tag2Bs). More detailed description of the modifications made in T7Syn-17Tag2Bs can be found in Figure S2.

Using the extracted genomic DNA as backbone, we swapped in a copy of the T7Syn Gp17 that has been tagged with a 19bp barcode capable of distinguishing up to 10^9 unique variants (T7Syn-17Tagged). An analysis of GG efficiency showed that around 30% of the input DNA had been converted into completed product (Figure S3). Following TXTL, 10^7 pfus were obtained from the reaction. We pooled all the plaques and sequenced the barcodes by NGS. The result indicates that there were 10^7 unique variants in our pooled sample, suggesting that under our reaction condition, the pfu obtained after TXTL is a true representation of library diversity.

Evolving host specificity by tail fiber mutagenesis

It has been reported in previous works that grafting a T3 phage tail fiber onto T7 will confer the latter with the host range of T3 phage [10,11]. T3 phage can form plaques only on *Escherichia coli* B strains whereas T7 phage can form plaques on both *E. coli* B and K12 strains. As a proof-of-concept, we wanted to see if we can evolve the T3 tail fiber of a T7/T3 hybrid phage to regain the ability to form plaques on *E. coli* K12 strains.

Using T7Syn-17Bs as the backbone, we swapped in the T3 tail fiber from amino acid position 176 up to its stop codon. In agreement with previous studies, we found that the resulting T7Syn-17T3 hybrid can indeed achieve a complete specificity switch, achieving an efficiency of plating (EOP) of $<10^{-7}$ on *E. coli* MG1655, a K12 strain compared to *E. coli* BL21, a B strain (Figure 3A). We then reintroduced *Bsa*I sites to T7Syn-17T3 and swapped in a library of randomly mutagenized 17T3 tail fiber variants each with 5-8 random nucleotide substitutions. The mutagenized phage was rebooted by TXTL, resulting in a titer of around 10^6 pfu/12 µL TXTL on BL21. For mutagenized libraries, pfu measurements will always underestimate the true titer of the reaction, because mutants that have lost the ability to invade BL21 will not show up in the pfu count. We plated dilutions of the TXTL reaction onto a lawn of MG1655 at a density where individual plaques could be picked. Mutants that could form large clear plaques on MG1655 could be obtained readily. We estimate that the rate of positive gain-of-function mutations was close to 1%. Sequencing of the positive mutants revealed that these mutants have between 3 to 5 amino acid changes within Gp17, and have unchanged Gp11 and Gp12. Our small sampling of 4 positive mutant sequences did not reveal any consensus mutations. The observed mutation rate was within the expected range of our mutagenesis library.

The gain-of-function phenotype was so easily obtainable that we could pick up some positive mutants from the negative control, where we swapped in an unmutated 17T3 tail fiber (Figure 3B). Sequencing of these positive mutants from the negative control revealed that these mutants have only one amino acid change within either Gp17 or Gp12, and are most likely the result of PCR error or replication error. This shows that T3 to T7 host range switch requires only a single nucleotide change. In this instance, T3 to T7 host range extension was found to only require small evolutionary steps. To challenge the platform, we next tested its ability to bridge bigger evolutionary gaps.

Testing the limits of directed evolution

To select potential targets, we tested a panel of 47 strains for their susceptibility towards wild-type T7 phage, and eliminated those that were found to be fully susceptible in a liquid lysis assay (Figure 1E, Figure S4). Twenty non-susceptible strains were selected for further testing using a plate-based titer assay where serially diluted T7 phages were dotted onto a lawn of bacteria. Three strains showed zones of inhibition at high T7 concentrations above 10^7 pfu/mL – *Salmonella enterica* ATCC#29630, *Salmonella enterica* ATCC#51741, and *Yersinia*

enterocolitica (YE) ATCC#23715 (Figure 3C, Supplemental Figure S5). Other than these 3 strains that appeared to be mildly susceptible, we selected based on their clinical significance, another 9 non-susceptible strains including enterohemorrhagic *E. coli*, *Acinetobacter baumannii*, *Pseudomonas putida*, *Citrobacter braakii*, *Citrobacter freundii*, *Shigella sonnei*, and *Shigella flexneri*. All in all, 12 strains were selected for the screening of our T7 gp17 mutagenesis library (Figure S6).

Random mutagenesis libraries (5-8 nt changes per gene) of Gp17, Gp11-12, and Gp11-12/Gp17 double mutant were generated from T7Syn-17Bs, T7Syn-1112Bs, and T7Syn-111217Bs at an estimated Golden Gate efficiency of 30%, 30%, and 9% respectively. After TXTL reboot, the resultant titer on BL21 was 10^6, 10^6, and 10^2 per 12 µL reaction. The reaction efficiency for double mutant was proximately the product of the single mutant reaction efficiencies. Given the low Golden Gate efficiency and the large sequence space, we believe that creating a large enough double mutant library is extremely challenging. Double mutant libraries were therefore excluded from the subsequent experiments.

We plated at least 5×10^5 pfu of Gp17 mutants and at least 5×10^3 Gp11-12 mutants separately onto lawns of the 12 strains we identified for screening. The Gp17 mutant library formed hundreds of small plaques on YE, while plating a similar number of T7wt phage or T7Syn phage did not result in any plaque (Figure 3D). Eight plaques were picked from the initial YE plate, resuspended in 200 µL phosphate buffered saline to make plaque stocks, which were then titered on a fresh lawn of YE, *E. coli* K-12 (MG1655), and *Yersinia pseudotuberculosis* IP2666. The plaque stocks of 8 different plaque isolates showed variable levels of plaque-forming activity towards YE, while they all showed consistent plaque-forming activity towards K12 and IP2666 (Figure 3E, only 4 shown). The plaque stock titers on K12 and IP2666 were around 10^8 pfu/mL, and the titers on YE were around 100-fold less. To ensure homogeneity, mutants that showed clear plaque-forming activity were re-isolated twice by plating at low density (~100 pfu/plate) and plaque picking. The best mutant based on titer and plaque appearance, T7Syn-17m5, contains 4 amino acid changes in Gp17. T7Syn-17m5 forms small (1-2 mm) clear plaques on BL21, MG1655, and YE, and is capable of liquid lysis (Figure 3F). The mutant libraries did not form plaques on the other strains we screened (Figure S6). Our results indicate that the strains that can be targeted by mutagenesis is limited to closely related species.

Improving Yersinia lysis efficiency through directed evolution

While evolving new specificity turned out to be extremely challenging, we hypothesized that improving a weak phage should be a more amenable problem. For this, we tried to improve the lytic activity of phages through mutagenesis of the tail components. We started with T7Syn-17m5 phage that we had picked up from the earlier screen, and we wanted to see if we could further improve its activity towards YE through a second round of mutagenesis.

Preparation of the mutagenesis libraries was performed in a manner similar to previous examples – we reintroduced *Bsa*I sites flanking the region of interest, then we swapped in a mutagenized copy into the phage genomic DNA through Golden Gate reaction. We created two libraries for each of the two phages, one for Gp11-12 and another for Gp17. The rebooted phage libraries were plated onto a lawn of target bacteria, and we picked the 8 biggest and clearest plaques for further characterization.

For T7Syn-17m5, second-round mutagenesis of Gp17 did not result in any significant improvement on its YE lysis performance, based on both plaque titer and liquid lysis assay. However, one of the selected second-round Gp17 mutants, T7Syn-5m7 showed decreased lysis performance towards BL21 while maintaining similar lysis performance against YE (Figure 3F and G). The decoupling of the activity towards YE and BL21 suggests that it might be possible to shift specificity away from BL21 to eventually achieve a host range switch instead of host range broadening. Although further mutagenesis of Gp17 did not result in significant improvement on YE lysis, mutagenesis of Gp11-12 did improve YE lysis. Using T7-Syn17m5 as the parent, mutagenesis of Gp11-12 resulted in a variant, T7Syn-12m1, that showed faster lysis time than T7Syn-17m5 (Figure 3F). Sequencing analysis showed that T7Syn-12m1 has a single amino acid change within Gp12 (Figure S1).

Interestingly, T7Syn-17m5 and T7Syn-5m7 both showed resistance suppression in BL21 (Figure 3H). After prolonged incubation with phages, BL21 started to develop resistance towards T7wt and T7Syn, and a resistant culture regrew after 8 hours. T7Syn-17m5 and T7Syn-5m7 were able to suppress the rise of resistance for at least 12 hours.

Improving Klebsiella lysis efficiency through directed evolution

To test the generalizability of this directed evolution strategy, we tried to improve the lysis performance of a K11 bacteriophage tail fiber towards *Klebsiella sp. 390* (K390). K11 Gp11,

12, 17 homologues were amplified in fragments to remove *Bsa*I and *Esp3*I restriction sites, pre-assembled in two plasmids by Golden Gate assembly, and sequence verified. These recoded tail components were then used to replace their T7 homologues to create two versions of T7-K11 hybrid phage. T7Syn-K111217 contain a complete swap of Gp11, Gp12, and Gp17, whereas T7Syn-TK17 contain a partial swap of gp17 from amino acid position 169 up to its stop codon, as well as a mutagenized copy of T7Gp11-12 (Figure 4A).

In agreement with previous observations, T7Syn-K111217 could form plaques on K390 [10,11]. In addition, we also found that T7Syn-TK17 could form plaques on K390 too (Figure 4B). This showed that K11Gp11-12 were not necessary for T7 phage to acquire the ability to lyse K390. Slight modification of T7Gp11-12 was sufficient to complement the TK17 hybrid tail fiber to enable K390 lysis. Intriguingly, we observed that both T7Syn-K111217 and T7Syn-TK17's activity towards K390 were highly media-dependent. Both phages were able to lyse K390 grown in nutrient broth (NB) efficiently, but fail to lyse K390 grown in lysogeny broth (LB) (Figure 4C and D). We wanted to see if we could improve its activity towards K390 in LB through mutagenesis.

Mutagenesis was carried out on K11Gp11-12, K11Gp17 as described in the previous section. The mutagenized phage libraries were screened on K390 grown in LB and the 8 biggest and clearest plaques were picked for further analysis. From these plaques, we isolated mutants that showed markedly improved lysis performance on K390 grown in LB. The best mutant, T7Syn-KmL2, could effect liquid lysis in a K390 LB culture, whereas T7Syn-K111217 and T7Syn-TK17 could not (Figure 4C and D). On plaque forming assay, T7Syn-17KmL2 formed clear plaques while the parents formed hazy plaques. Sequencing revealed that the improved phenotype is conferred by a single amino acid change in K11 Gp17 within the T7Syn-K111217 variant. Unfortunately, plating the T7-K11 hybrid mutagenesis libraries on other Klebsiella strains that are resistant to K11 phage, such as *Klebsiella oxytoca* and *Klebsiella pneumoniae*, did not result in any plaque formation.

DISCUSSION

In this study, we have demonstrated the speed and flexibility of our phage engineering platform using T7 phage. However, this strategy should be applicable to many other dsDNA phages. Since no attachment, invasion, and lysis is necessary for phage assembly in cell-free

transcription translation (TXTL), the engineered phages do not need to retain their activity towards *E. coli* or any particular host. The only requirement for this platform is that the transcription and translation machineries must be compatible to that of *E. coli*. This limitation can most likely be overcome through the development of TXTL reactions that are based on the lysate from the species of interest.

As phage and their host have coevolved over millions of years, they have become incredibly diverse. As a result, the evolutionary distance between far away lineages is way beyond the reach of random mutagenesis [18]. For example, the K11 tail fiber is almost twice as big as that of T7, and it contains a catalytic domain that can digest bacterial capsule [19,20]. It is extremely unlikely that such functionality can be obtained through random mutagenesis, thereby limiting the targetable strains to only closely related species. There is a sweet spot for new host adaptation – being too close would make the host susceptible to the parent phage, being too far would make the host unreachable by one-step evolution. For example, *Yersinia pestis* is very closely related to *E. coli* K-12, [21], and we found that *Y. pseudotuberculosis* IP2666, a strain most closely related to *Y. pestis*, is fully susceptible to T7 phage [22]. We were not able to test *Yersinia pestis* due to regulatory limitations. *Yersinia enterocolitica* is slightly further from *Y. pestis*, and is highly resistant towards T7 phage. *Y. enterocolitica* turned out to be within the sweet spot, and we could evolve the parent phage to overcome the resistance. Given the limitations on the bridgeable evolutionary distance, we expect the main application of directed evolution will be to target closely related strains, such as the resistant strains that have been derived from a susceptible parent strain.

One key limitation of our study, that we have realized only during peer review, is that the tail fibers and the packaged genome became unlinked during TXTL, which has made the direct screening from TXTL ineffective. While direct screening could be used for the mutagenesis of components, such as the kinases, nucleases and polymerases, that are expressed after host entry, direct screening of structural components should have been avoided. The linkage between structural components and the packaged genome could be restored either by performing TXTL under microencapsulation [23,24], or by allowing one round of lysis in the native host. Given the limitation, we can only expect our screen to work on strains that are mildly susceptible to the wild-type phage. It is not a good gauge of the evolutionary distance bridgeable by random mutagenesis. We will address this limitation in a follow-up study.

Another limitation is that plaque appearance screening is most effective for detecting mutants that have improved from non-plaque forming to plaque forming. When the parent phage is non-plaque forming, we can plate 10^6 mutant phages on one plate and will still be able to pick up the few that are able to form plaques. However, when the parent is plaque forming, we can only fit 10^3 mutant phages on one plate before the plaque density becomes too high to detect the few clearer or bigger plaques. As a result, further rounds of mutagenesis are unlikely to result in marked improvement once the phage becomes plaque forming.

Recently, Yehl et al. reported the use of tail fiber mutagenesis to expand the host range of tailed phages [13]. They proposed that there are variable loop regions on the tail fiber that are important for host specificity. Focusing the mutagenesis on these smaller regions can potentially make our screening more effective. However, it is worth noting that for T7Syn-17m5 that has acquired the ability to attack YE, all 4 amino acid changes reside outside the variable loop regions. We also found that while Gp17 is important for acquiring new targeting specificity, Gp11-12 is important for making the process efficient. Because Yehl et al. relied on recombination within a susceptible host to generate the phage library, it requires that the resultant library, however diverse, must retain their specificity towards the native host. Variants that resulted in a complete switch in specificity will be lost. We believe that our library preparation method, when done with microencapsulated TXTL, will complement the findings by Yehl et al., and allows for the generation of large phagebody libraries without the backward compatibility requirement.

Lastly, when it comes to engineering lytic growth in new hosts, it is important to look beyond the tail components. As Yosef et al. have pointed out in their study, phages can deliver DNA to many more hosts than they can replicate in [11]. This suggests that other means of phage resistance might be more important than phage attachment [25]. Engineering the host inhibition and host lysis components may enable lytic growth in many more hosts than engineering tail components alone. However, a method to quickly identify the bottleneck in the lytic growth cycle needs to be developed.

In summary, by directly assembling the full phage genome from PCR fragments, we have circumvented many limitations associated with yeast and cell-based assembly systems. This platform allows for the extensive re-engineering of dsDNA phage and for the creation of high diversity mutagenesis libraries. With a large library of recoded phages, it will be possible to

curate a collection of modular compatible phage parts, where we can have ready-to-use host inhibition module, DNA replication module, packaging module, host invasion module, and host lysis module. This platform should help propel phage engineering into the synthetic biology era, where we can pick and choose functionality modularly to target specific organisms. In the near future, we can look forward to the emergence of highly effective therapeutic phages that are evolved in the lab, and may even have properties that preclude its existence in nature.

METHODS

Assembly of chemically synthesized genome

The entire T7 phage genome were chemically synthesized by Genscript (Piscataway, NJ) in 14 fragments. The first 7 fragments approximately corresponding to the first half of the T7 genome were toxic in *E. coli*, and had to be carried on yeast plasmid vector instead of pUC vector. For assembly, 14 PCR fragments containing compatible *Bsa*I junctions were prepared and subsequently assembled into a complete genome via a 1-step Golden Gate (GG) reaction. After DNA precipitation, the GG product was used to produce live phages via a cell-free transcription translation (TXTL) reaction [26]. The full list of constructed phage variants can be found in Figure S1.

Golden Gate Assembly

The Golden Gate assembly method has been adapted from Engler et al. and optimized in this work to achieve high efficiency assembly [27]. Two µg of purified PCR fragments, in 1:1 molar ratio, were used in a 20 µL GG reaction. All enzymes were obtained from New England Biolabs (Ipswich, MA). The reaction was set up with 2 µL T4 DNA Ligase reaction buffer, 0.4 µL high concentration T4 DNA Ligase (NEB #M0202M), 1.6 µL *Bsa*I-HFv2 (NEB #R3733L), made up to 20 µL with DNA fragments and water. Reactions were carried out on a thermocycler using the following cycle: (1) 37ºC 10min, (2) 37ºC 10min, (3) 14ºC 6min, (4) Goto (2) for 40X, (5) 14ºC 15min, (6) 37ºC 15min, (7) 80ºC 5min, (8) 10ºC hold. To prepare for TXTL reboot, the GG reaction was precipitated by isopropanol [28] and dissolved in 2 µL water. The number of cycles can be reduced to 20X for simpler assemblies or when library-efficiency is not required. Scaling down of the reaction is not recommended as DNA precipitation becomes more difficult.

Rebooting of assembled phage genome by cell-free transcription translation (TXTL)

TXTL reaction was done using either myTXTL Sigma 70 Master Mix Kit + GamS or myTXTL Linear DNA Expression Kit from Arbor Biosciences (Ann Arbor, MI) according to manufacturer's recommendations. Briefly, each 12 µL myTXTL Sigma70 reaction consisted of 9 µL myTXTL mix, 0.8 µL 150µM GamS, 0.36 µL 10mM dNTP, 0.75 µL 40% PEG-8000, and up to 1.09 µL re-dissolved DNA. Condition for myTXTL Linear DNA kit was similar except that GamS was not needed, and up to 1.89 µL re-dissolved DNA could be added. Reactions were incubated at 29ºC for 16 hours and then titered to determine pfu yield. Both kits resulted in efficient live phage production.

Phage genomic DNA purification

Phage genomic DNA were typically prepared from 40 mL of 0.45 µm filtered phage lysate. Bacterial DNA/RNA were digested by adding $MgSO_4$, $CaCl_2$, DNase I, and RNase A to at 5 mM, 0.5 mM, 5 U/mL, and 5µg/mL final concentration respectively, and incubated at 37 ºC for 90 minutes. Phage particles were concentrated by precipitation and resuspension. Briefly, solid PEG-8000 and NaCl were added to 10% w/v and 1M respectively followed by overnight incubation at 4ºC. Precipitates were pelleted by centrifugation at 15,000 ×g, 4ºC for 20 minutes. After the complete removal of supernatant, the phage pellet was resuspended in 500 µL resuspension buffer (10 nM Tris pH7.4, 2.5 mM $MgSO_4$, 0.5 mM $CaCl_2$), and insoluble matter was removed by centrifugation at 10,000 ×g, 4ºC for 3 minutes. Remnant nucleases were inactivated by adding EDTA and proteinase K to 10 mM and 0.25 mg/mL respectively, and incubated at 50ºC for 15 minutes. DNA were then purified via phenol-chloroform extraction followed by isopropanol precipitation.

Verification of library size by barcode tag analysis

Barcoded phage libraries were generated by GG and rebooted by TXTL. The entire rebooted phage library was plated on 5 × 100 mm MG1655 lawns, plaques were washed off the plates, and their genomic DNA were purified from the wash. Using the genomic DNA as template, two PCR of 10 cycles each were sequentially performed to amplify the tag and to attach NGS adapters to them. After gel purification, the amplicon library was sequenced on HiSeq using SE50 chemistry. Raw data output was 1.66×10^8 reads, and the raw data was analyzed using Galaxy [29]. Detail results of the analysis can be found on Figure S7.

Random mutagenesis

Random mutagenesis was performed using GeneMorph II Random Mutagenesis Kit from Agilent (Santa Clara, CA). The target mutation rate was 5-8 nt changes per gene, and it could be achieved for smaller amplicons, such as T7 Gp17, using manufacturer's recommendation. For the larger amplicons, such as T7 Gp11-12 and K11 Gp17, modifications to manufacturer's protocol were necessary. Briefly, a 1:1 mixture of *Taq* and Mutazyme II DNA polymerase were used, so as to lower the mutation rate without using excessive template. Clones from the mutagenized libraries were sequenced by Sanger sequencing to verify the mutation rate. Full list of engineered mutant phage can be found in Figure S1.

Liquid lysis assay

Bacterial strains were grown overnight to saturation in their respective culture media and condition. Saturated culture were diluted 1:50 and allowed to recover to log-phase for 2 hours. Log-phase culture were further diluted 1:10 and 200µL of the diluted culture were added to each well in a transparent flat-bottom 96 well plate. The OD was then recorded at 2 minutes interval in a plate reader, at culture temperature with intermittent shaking. When growth was re-established, in approximately 10 minutes, up to 10 µL plaque or phage stocks were added to each well, and the plate was returned to the plate reader to continue the OD recording. For susceptibility measurement, high titer ($>10^{10}$ pfu/mL) phage stocks were used to achieve a high multiplicity of infection (MOI) (>5). Burst time was determined using data from the point of phage addition, and it was defined as the time when the largest change in OD occurred. The burst timing was found to be independent of MOI, but a MOI at around 0.5 tended to make two lysis cycles visible, adding to the confidence of lysis timing. List of bacterial strains and their respective culture condition can be found in Figure S4.

AUTHOR CONTRIBUTIONS

JL and HBZ conceptualized the study; JL, HBZ, and YLT performed the experiments; JL, HMZ, and ELA analyzed the data; JL, HMZ, and ELA wrote and revised the manuscript.

CONFLICTS OF INTEREST

None

ACKNOWLEDEMENT

Bacteriophage K11, *Klebsiella* sp. 390, and *Yersinia tuberculosis* IP2666 were kind gifts from Timothy K. Lu, Massachusetts Institute of Technology. This work was supported by HBMS

IAF-PP grant (H17/01/a0/0V9) and A*STAR Visiting Investigator Program (1535j00137 to H.Z).

SUPPORTING INFORMATION

REFERENCES

(1) Review on Antimicrobial Resistance. (2014) Antimicrobial Resistance: Tackling a Crisis for the Future Health and Wealth of Nations.

(2) Sugden, R., Kelly, R., and Davies, S. (2016) Combatting antimicrobial resistance globally. *Nat. Microbiol. 1*, 16187.

(3) Salmond, G. P. C., and Fineran, P. C. (2015) A century of the phage: past, present and future. *Nat. Rev. Microbiol. 13*, 777–786.

(4) Czaplewski, L., Bax, R., Clokie, M., Dawson, M., Fairhead, H., Fischetti, V. A., Foster, S., Gilmore, B. F., Hancock, R. E. W., Harper, D., Henderson, I. R., Hilpert, K., Jones, B. V., Kadioglu, A., Knowles, D., Ólafsdóttir, S., Payne, D., Projan, S., Shaunak, S., Silverman, J., Thomas, C. M., Trust, T. J., Warn, P., and Rex, J. H. (2016) Alternatives to antibiotics—a pipeline portfolio review. *Lancet Infect. Dis. 16*, 239–251.

(5) Kortright, K. E., Chan, B. K., Koff, J. L., and Turner, P. E. (2019) Phage Therapy: A Renewed Approach to Combat Antibiotic-Resistant Bacteria. *Cell Host Microbe 25*, 219–232.

(6) Schmidt, C. (2019) Phage therapy's latest makeover. *Nat. Biotechnol. 37*, 581–586.

(7) Dedrick, R. M., Guerrero-Bustamante, C. A., Garlena, R. A., Russell, D. A., Ford, K., Harris, K., Gilmour, K. C., Soothill, J., Jacobs-Sera, D., Schooley, R. T., Hatfull, G. F., and Spencer, H. (2019) Engineered bacteriophages for treatment of a patient with a disseminated drug-resistant Mycobacterium abscessus. *Nat. Med. 25*, 730–733.

(8) Schooley, R. T., Biswas, B., Gill, J. J., Hernandez-Morales, A., Lancaster, J., Lessor, L., Barr, J. J., Reed, S. L., Rohwer, F., Benler, S., Segall, A. M., Taplitz, R., Smith, D. M., Kerr, K., Kumaraswamy, M., Nizet, V., Lin, L., McCauley, M. D., Strathdee, S. A., Benson, C. A., Pope, R. K., Leroux, B. M., Picel, A. C., Mateczun, A. J., Cilwa, K. E., Regeimbal, J. M., Estrella, L. A., Wolfe, D. M., Henry, M. S., Quinones, J., Salka, S., Bishop-Lilly, K. A., Young, R., and Hamilton, T. (2017) Development and Use of Personalized Bacteriophage-Based Therapeutic Cocktails To Treat a Patient with a Disseminated Resistant Acinetobacter baumannii Infection. *Antimicrob. Agents Chemother. 61*, e00954-17, /aac/61/10/e00954-17.atom.

(9) Oechslin, F. (2018) Resistance Development to Bacteriophages Occurring during Bacteriophage Therapy. *Viruses 10*, 351.

(10) Ando, H., Lemire, S., Pires, D. P., and Lu, T. K. (2015) Engineering Modular Viral Scaffolds for Targeted Bacterial Population Editing. *Cell Syst. 1*, 187–196.

(11) Yosef, I., Goren, M. G., Globus, R., Molshanski-Mor, S., and Qimron, U. (2017) Extending the Host Range of Bacteriophage Particles for DNA Transduction. *Mol. Cell 66*, 721-728.e3.

(12) Dunne, M., Rupf, B., Tala, M., Qabrati, X., Ernst, P., Shen, Y., Sumrall, E., Heeb, L., Plückthun, A., Loessner, M. J., and Kilcher, S. (2019) Reprogramming Bacteriophage Host Range through Structure-Guided Design of Chimeric Receptor Binding Proteins. *Cell Rep. 29*, 1336-1350.e4.

(13) Yehl, K., Lemire, S., Yang, A. C., Ando, H., Mimee, M., Torres, M. D. T., de la Fuente-Nunez, C., and Lu, T. K. (2019) Engineering Phage Host-Range and Suppressing Bacterial Resistance through Phage Tail Fiber Mutagenesis. *Cell 179*, 459-469.e9.

(14) Bassalo, M. C., Liu, R., and Gill, R. T. (2016) Directed evolution and synthetic biology applications to microbial systems. *Curr. Opin. Biotechnol. 39*, 126–133.

(15) Cobb, R. E., Chao, R., and Zhao, H. (2013) Directed evolution: Past, present, and future. *AIChE J. 59*, 1432–1440.

(16) Molina-Espeja, P., Viña-Gonzalez, J., Gomez-Fernandez, B. J., Martin-Diaz, J., Garcia-Ruiz, E., and Alcalde, M. (2016) Beyond the outer limits of nature by directed evolution. *Biotechnol. Adv. 34*, 754–767.

(17) Pryor, J. M., Potapov, V., Pokhrel, N., and Lohman, G. J. S. (2020) Rapid 40 kb genome construction from 52 parts. *bioRxiv* 2020.12.22.424019.
(18) Grose, J. H., and Casjens, S. R. (2014) Understanding the enormous diversity of bacteriophages: The tailed phages that infect the bacterial family Enterobacteriaceae. *Virology 468–470*, 421–443.
(19) Bessler, W., Freund-Mölbert, E., Knüfermann, H., Rudolph, C., Thurow, H., and Stirm, S. (1973) A bacteriophage-induced depolymerase active on Klebsiella K11 capsular polysaccharide. *Virology 56*, 134–151.
(20) Latka, A., Maciejewska, B., Majkowska-Skrobek, G., Briers, Y., and Drulis-Kawa, Z. (2017) Bacteriophage-encoded virion-associated enzymes to overcome the carbohydrate barriers during the infection process. *Appl. Microbiol. Biotechnol. 101*, 3103–3119.
(21) Deng, W., Burland, V., Plunkett III, G., Boutin, A., Mayhew, G. F., Liss, P., Perna, N. T., Rose, D. J., Mau, B., Zhou, S., Schwartz, D. C., Fetherston, J. D., Lindler, L. E., Brubaker, R. R., Plano, G. V., Straley, S. C., McDonough, K. A., Nilles, M. L., Matson, J. S., Blattner, F. R., and Perry, R. D. (2002) Genome Sequence of Yersinia pestis KIM. *J. Bacteriol. 184*, 4601–4611.
(22) Ibrahim, A., Goebel, B. M., Liesack, W., Griffiths, M., and Stackebrandt, E. (1993) The phylogeny of the genus *Yersinia* based on 16S rDNA sequences. *FEMS Microbiol. Lett. 114*, 173–177.
(23) Saeki, D., Sugiura, S., Kanamori, T., Sato, S., and Ichikawa, S. (2014) Microcompartmentalized cell-free protein synthesis in semipermeable microcapsules composed of polyethylenimine-coated alginate. *J. Biosci. Bioeng. 118*, 199–204.
(24) Spencer, A. C., Torre, P., and Mansy, S. S. (2013) The Encapsulation of Cell-free Transcription and Translation Machinery in Vesicles for the Construction of Cellular Mimics. *J. Vis. Exp.* 51304.
(25) Labrie, S. J., Samson, J. E., and Moineau, S. (2010) Bacteriophage resistance mechanisms. *Nat. Rev. Microbiol. 8*, 317–327.
(26) Rustad, M., Eastlund, A., Marshall, R., Jardine, P., and Noireaux, V. (2017) Synthesis of Infectious Bacteriophages in an E. coli-based Cell-free Expression System. *J. Vis. Exp.* 56144.
(27) Engler, C., Kandzia, R., and Marillonnet, S. (2008) A One Pot, One Step, Precision Cloning Method with High Throughput Capability. *PLoS ONE* (El-Shemy, H. A., Ed.) *3*, e3647.
(28) Green, M. R., and Sambrook, J. (2017) Precipitation of DNA with Isopropanol. *Cold Spring Harb. Protoc. 2017*, pdb.prot093385.
(29) Afgan, E., Baker, D., Batut, B., van den Beek, M., Bouvier, D., Čech, M., Chilton, J., Clements, D., Coraor, N., Grüning, B. A., Guerler, A., Hillman-Jackson, J., Hiltemann, S., Jalili, V., Rasche, H., Soranzo, N., Goecks, J., Taylor, J., Nekrutenko, A., and Blankenberg, D. (2018) The Galaxy platform for accessible, reproducible and collaborative biomedical analyses: 2018 update. *Nucleic Acids Res. 46*, W537–W544.

585 **Figure legends**

586

587 Figure 1. Complete chemical synthesis and rebooting of Golden Gate compatible T7 phage.
588 (A) General scheme of assembly, from a user designed genomic sequence to live phage. (B)
589 Gel electrophoresis of PCR products amplified from phage plaques (Uncut). Syn1 through
590 Syn8 were amplified from 8 randomly selected T7Syn plaques after assembly and reboot, T7
591 was amplified from T7wt gDNA, and Ctr1 through Ctr3 were amplified from plaques of
592 rebooted T7wt gDNA. The PCR products were then digested using *Bsa*I, and analyzed on a
593 separate gel (*Bsa*I Cut). (C) Lysates of T7wt and T7Syn titered on BL21 by serial dilutions,
594 lowest dilution was 10^{-7}. T7wt and T7Syn resulted in similar titers. (D) Burst time comparison
595 between T7wt and T7Syn. Rate of change of OD is plotted against time, and the burst time is
596 defined as the time with the largest OD decrease. Data for Syn has been plotted on secondary
597 axis for clarity. Error bar represents standard deviation of 3 replicates. (E) Liquid culture of
598 different bacterial strains challenged by T7Syn, T7wt, and T3wt phages. Results shown by
599 color scale represent the extent of lysis as indicated by a change in OD when compared to a
600 no-phage control of the same strain. A negative OD change represents lysis, a positive but
601 reduced OD change represents inhibition, and no difference from no-phage control represents
602 normal growth, i.e., complete resistance. Partial results (36 of 47 strains tested) shown here,
603 the full list can be found in Figure S4. Image Credit: Illustration of T7 bacteriophage has been
604 adapted from https://cronodon.com/BioTech/Virus_Tech_2.html with permission.

605

606 Figure 2. Functionalization and modification of T7Syn genome. (A) Schematic of T7Syn
607 modifications used for generating Gp17 random mutagenesis and Gp17 random tag libraries.
608 (B) Confirmation of *Bsa*I site insertions. Gel electrophoresis of *Bsa*I digested gDNA purified
609 from modified phages. Molecular marker was the NEB 1kb extended DNA ladder, the top band
610 is 48.5 kb and the dark band is 3 kb. a-e are the expected bands generated by *Bsa*I sites flanking
611 Gp11-12, in pink, or Gp17, in orange. (C) Burst time evaluation of the T7Syn variants. Rate of
612 change of OD is plotted against time, and the burst time is defined as the time with the largest
613 OD decrease. Error bar represents standard deviation of 3 replicates.

614

615 Figure 3. Evolving new host specificity. (A) Titering of T7Syn-17T3 lysate on *E. coli* BL21
616 (B strain) and MG1655 (K12 strain). The efficiency of plating was $< 10^{-7}$. (B) Titering of
617 plaque stocks on MG1655. T3m showed 4 randomly selected plaques of a rebooted T7Syn-
618 17T3 tail fiber random mutagenesis phage library, whereas T3c showed 4 randomly selected

plaques of a rebooted negative control with a wild-type T3 tail fiber swapped in. (C) Dilution of T7wt, T7Syn, and T3 phages titered on YE. Zones of inhibition is visible at high T7 and Syn concentration, but no individual plaque can be seen. (D) Plating of phages on YE for plaque isolation. Top: at least 3×10^5 pfu of Gp17 random mutagenesis phage library, many small but clearly visible plaques can be seen. Bottom: ~ 1×10^6 pfu of T7Syn phage, no plaque can be observed. (E) Titers of 4 randomly selected plaques isolated from Gp17 random mutagenesis phage library plated on YE. Top: plaque stock showed varying degree of activity against YE. Middle: plaque stocks retained full activity towards K12 strain. Bottom: plaque stocks were fully active against *Yersinia pseudotuberculosis* IP2666. (F) YE burst time comparison between the best performing first and second round variants. Rate of change of OD is plotted against time, and the burst time is defined as the time with the largest OD decrease. Error bar represents standard deviation of 3 replicates. Two separate bursts of lysis were clearly visible for 17m5 (1^{st} round mutant), 12m1 (2^{nd} round Gp11-12 mutant) and 5m7 (2^{nd} round Gp17 mutant), the 2^{nd} round mutant being slightly faster than the 1^{st} round mutant. No lytic activity towards YE was observed for unmutated T7wt phage. (G) and (H) Lysis of BL21 by the Gp17 mutants and their parent phages. OD is plotted against time. Error bar represents standard deviation of 3 replicates. (G) All variants and their parents completely lysed BL21 within the first hour. T7Syn-17m5 was more active than the parent phage, whereas T7Syn-5m7 was less active than parent phage. (H) Resistance against the parent phages led to an increase in OD by the 12^{th} hour. The rise of resistance was suppressed by both T7Syn-17m5 and T7Syn-5m7.

Figure 4. Mutagenesis of T7-K11 hybrids. (A) Schematic of T7Syn variants used for generating the T7-K11 hybrids. T7Syn-K1112K17 had its Gp11, Gp12, and Gp17 replaced by the homologous genes from K11 phage, *Bsa*I-inserted variants were also created to allow mutagenesis, T7Syn-TK17 had its Gp17 C-terminus replaced by that from K11 phage. (B) Titering of two completed TXTL reactions on K390. T7Syn-K1112K17, reassembled using a 5-fragment Golden Gate reaction, resulted in a titer of ~10^3 per µL. T7Syn-TK17, reassembled from a direct Golden Gate swap-in, resulted in a titer of ~10^6 per µL. These yields are typical for their respective assembly complexity. (C) and (D) Lysis of K390 by T7-K11 hybrid variants and their parent phages. OD is plotted against time. Error bar represents standard deviation of 3 replicates. T7Syn-KmL2 is an improved mutant isolated from a Gp11,12,17 random mutagenesis library plated on K390 in LB. (C) Lysis curve of K390 in NB. All variants could lyse K390 in NB. (D) Lysis curve of K390 in LB. Although the wild type K11 phage can lyse

652 K390 efficiently in LB, K390 in LB is much more resistant to lysis by the T7-K11 hybrids.
653 KmL2 showed marked improvement over its T7-K11 hybrid parents.

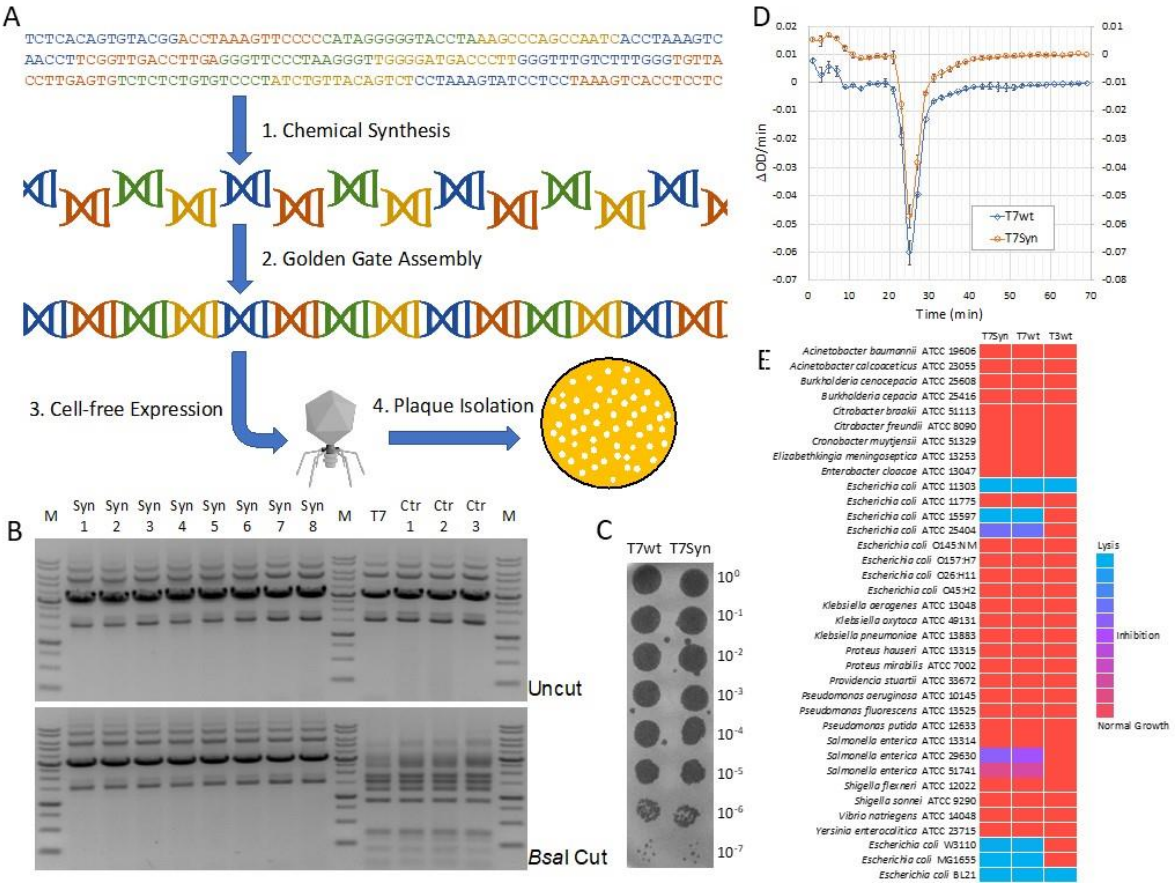
A
TCTCACAGTGTACGGACCTAAAGTTCCCCCATAGGGGGTACCTAAAGCCCAGCCAATCACCTAAAGTC
AACCTTCGGTTGACCTTGAGGGTTCCCTAAGGGTTGGGGATGACCCTTGGGTTTGTCTTTGGGTGTTA
CCTTGAGTGTCTCTCTGTGTCCCTATCTGTTACAGTCTCCTAAAGTATCCTCCTAAAGTCACCTCCTC
1. Chemical Synthesis
2. Golden Gate Assembly
3. Cell-free Expression
4. Plaque Isolation
B
M
Syn 1
Syn 2
Syn 3
Syn 4
Syn 5
Syn 6
Syn 7
Syn 8
M
T7
Ctr 1
Ctr 2
Ctr 3
M
Uncut
BsaI Cut
C
T7wt T7Syn
10^0
10^-1
10^-2
10^-3
10^-4
10^-5
10^-6
10^-7
D
ΔOD/min
Time (min)
T7wt
T7Syn
E
T7Syn T7wt T3wt
Acinetobacter baumannii ATCC 19606
Acinetobacter calcoaceticus ATCC 23055
Burkholderia cenocepacia ATCC 25608
Burkholderia cepacia ATCC 25416
Citrobacter braakii ATCC 51113
Citrobacter freundii ATCC 8090
Cronobacter muytjensii ATCC 51329
Elizabethkingia meningoseptica ATCC 13253
Enterobacter cloacae ATCC 13047
Escherichia coli ATCC 11303
Escherichia coli ATCC 11775
Escherichia coli ATCC 15597
Escherichia coli ATCC 25404
Escherichia coli O145:NM
Escherichia coli O157:H7
Escherichia coli O26:H11
Escherichia coli O45:H2
Klebsiella aerogenes ATCC 13048
Klebsiella oxytoca ATCC 49131
Klebsiella pneumoniae ATCC 13883
Proteus hauseri ATCC 13315
Proteus mirabilis ATCC 7002
Providencia stuartii ATCC 33672
Pseudomonas aeruginosa ATCC 10145
Pseudomonas fluorescens ATCC 13525
Pseudomonas putida ATCC 12633
Salmonella enterica ATCC 13314
Salmonella enterica ATCC 29630
Salmonella enterica ATCC 51741
Shigella flexneri ATCC 12022
Shigella sonnei ATCC 9290
Vibrio natriegens ATCC 14048
Yersinia enterocolitica ATCC 23715
Escherichia coli W3110
Escherichia coli MG1655
Escherichia coli BL21
Lysis
Inhibition
Normal Growth

Figure 1

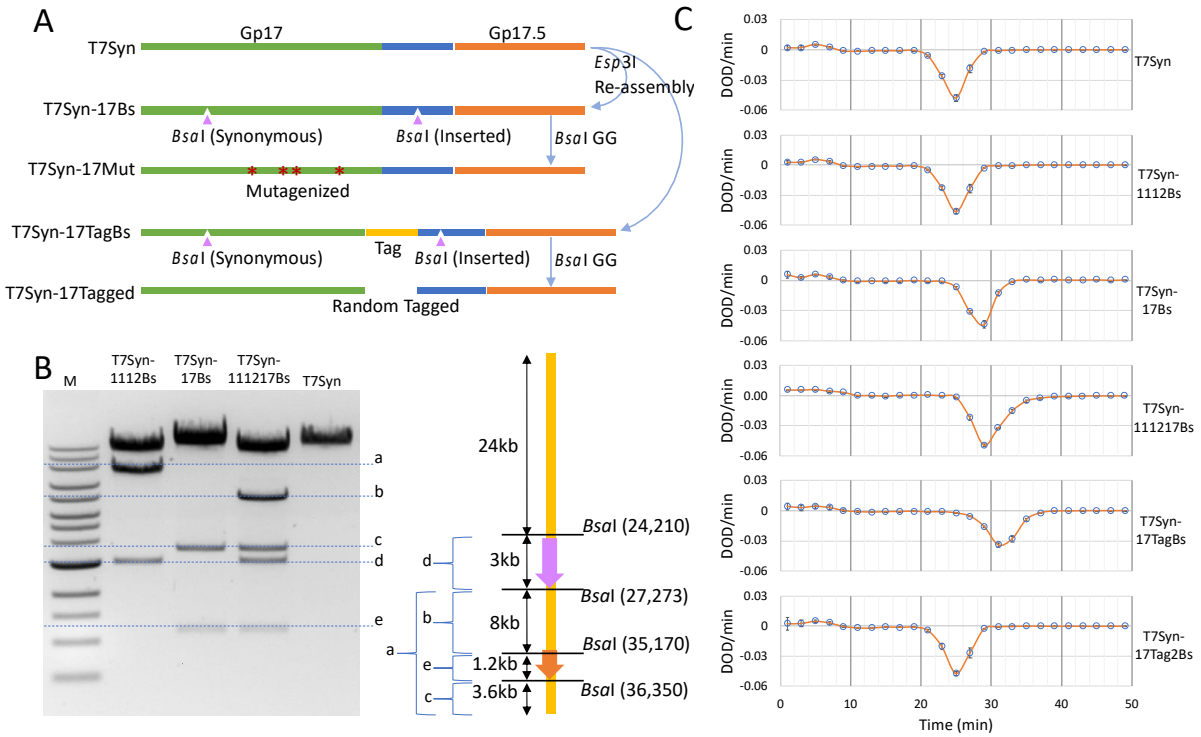
A
T7Syn
Gp17
Gp17.5
Esp3I
Re-assembly
T7Syn-17Bs
BsaI (Synonymous)
BsaI (Inserted)
BsaI GG
T7Syn-17Mut
Mutagenized
T7Syn-17TagBs
Tag
T7Syn-17Tagged
Random Tagged
B
M
T7Syn-1112Bs
T7Syn-17Bs
T7Syn-111217Bs
T7Syn
a
b
c
d
e
24kb
BsaI (24,210)
3kb
BsaI (27,273)
8kb
BsaI (35,170)
1.2kb
3.6kb
BsaI (36,350)
C
DOD/min
T7Syn
T7Syn-1112Bs
T7Syn-17Bs
T7Syn-111217Bs
T7Syn-17TagBs
T7Syn-17Tag2Bs
Time (min)

Figure 2

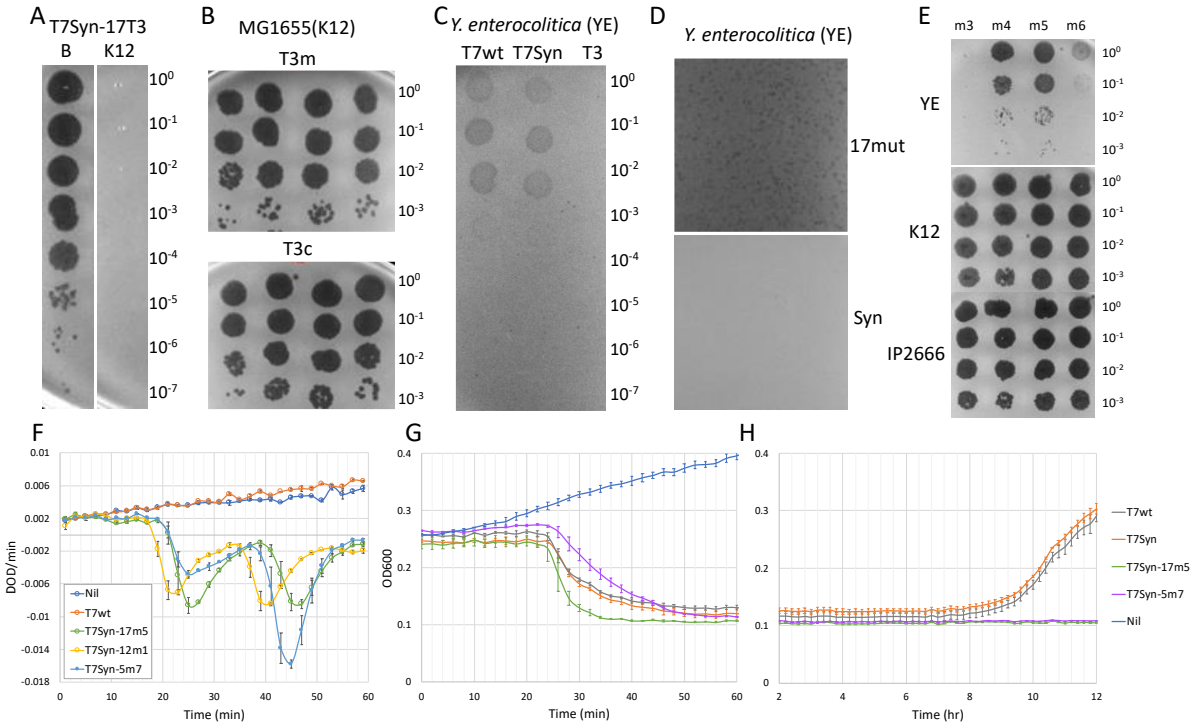
A
T7Syn-17T3
B
K12
B
MG1655(K12)
T3m
T3c
C
Y. enterocolitica (YE)
T7wt T7Syn T3
D
Y. enterocolitica (YE)
17mut
Syn
E
m3 m4 m5 m6
YE
K12
IP2666
F
DOD/min
Time (min)
Nil
T7wt
T7Syn-17m5
T7Syn-12m1
T7Syn-5m7
G
OD600
Time (min)
H
Time (hr)
T7wt
T7Syn
T7Syn-17m5
T7Syn-5m7
Nil

Figure 3

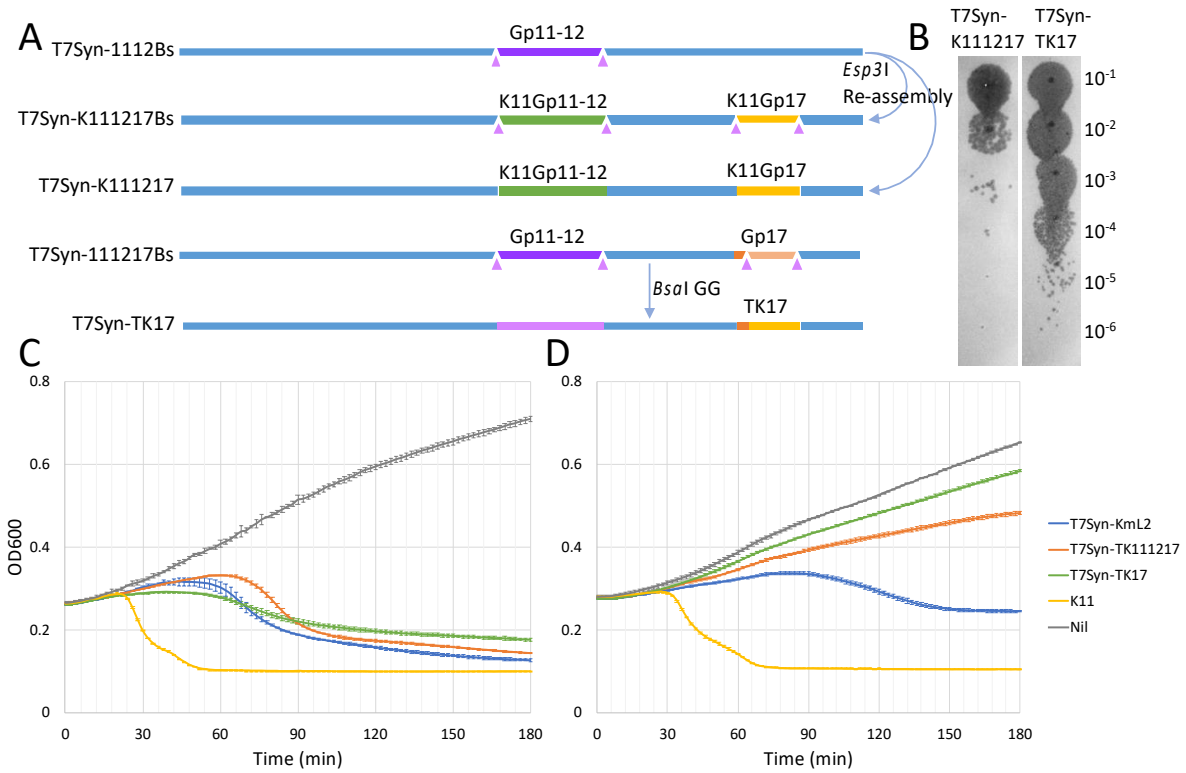
A
T7Syn-1112Bs
Gp11-12
T7Syn-K111217Bs
K11Gp11-12
K11Gp17
T7Syn-K111217
K11Gp11-12
K11Gp17
T7Syn-111217Bs
Gp11-12
Gp17
BsaI GG
T7Syn-TK17
TK17
Esp3I
Re-assembly
B
T7Syn-K111217
T7Syn-TK17
10-1
10-2
10-3
10-4
10-5
10-6
C
D
OD600
Time (min)
T7Syn-KmL2
T7Syn-TK111217
T7Syn-TK17
K11
Nil

Figure 4

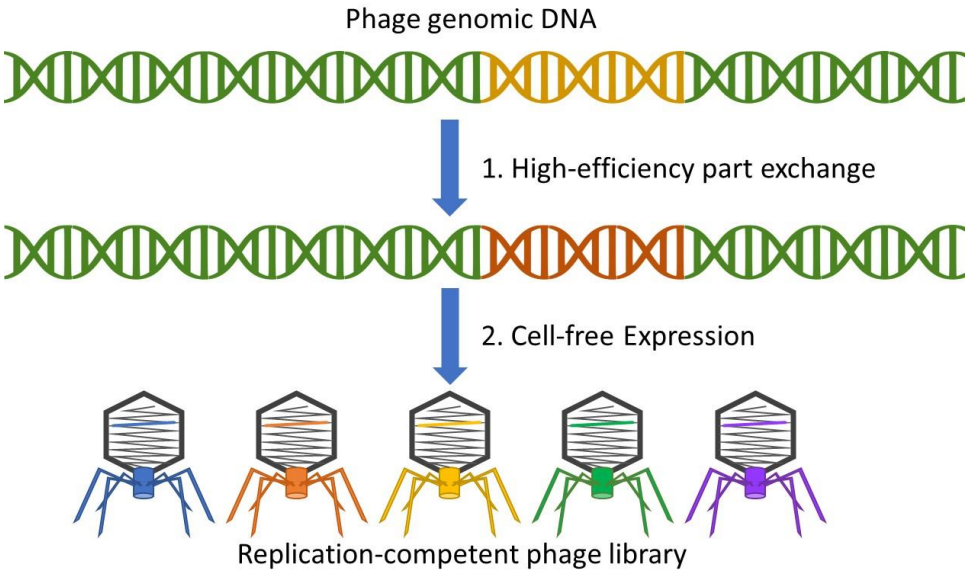

669

670 Table-of-Content Graphic